



HAL
open science

Performance analysis of the optimal widely linear MVDR beamformer

Pascal Chevalier, Jean-Pierre Delmas, Abdelkader Oukaci

► **To cite this version:**

Pascal Chevalier, Jean-Pierre Delmas, Abdelkader Oukaci. Performance analysis of the optimal widely linear MVDR beamformer. Eusipco 2009: 17th European Signal Processing Conference, Aug 2009, Glasgow, United Kingdom. pp.587 - 591. hal-01368943

HAL Id: hal-01368943

<https://hal.science/hal-01368943>

Submitted on 20 Sep 2016

HAL is a multi-disciplinary open access archive for the deposit and dissemination of scientific research documents, whether they are published or not. The documents may come from teaching and research institutions in France or abroad, or from public or private research centers.

L'archive ouverte pluridisciplinaire **HAL**, est destinée au dépôt et à la diffusion de documents scientifiques de niveau recherche, publiés ou non, émanant des établissements d'enseignement et de recherche français ou étrangers, des laboratoires publics ou privés.

PERFORMANCE ANALYSIS OF THE OPTIMAL WIDELY LINEAR MVDR BEAMFORMER

Pascal Chevalier¹, Jean-Pierre Delmas² and Abdelkader Oukaci³

¹ Thales-Communications, EDS/SPM, 92704 Colombes, France
pascal.chevalier@fr.thalesgroup.com

^{2,3} TELECOM SudParis, CNRS UMR 5157, 91011 Evry, France
jean-pierre.delmas(abdelkader.oukaci)@it-sudparis.eu

ABSTRACT

This paper presents a comprehensive performance analysis of the optimal widely linear (WL) minimum variance distortionless response (MVDR) beamformer for the reception of an unknown signal of interest (SOI) corrupted by potentially second order (SO) noncircular background noise and interference. The SOI, whose waveform is unknown, is assumed to be SO noncircular with arbitrary noncircularity properties. In the steady state and for SO noncircular SOI and/or interference, this WL beamformer is shown to always improve the signal to interference plus noise ratio (SINR) and the symbol error rate (SER) performance at the output of both the well-known Capon's beamformer and a WL MVDR beamformer introduced recently in the literature.

1. INTRODUCTION

Conventional beamforming approaches aim at finding a linear and time invariant (TI) complex filter \mathbf{w} , such that its output $y(t) \stackrel{\text{def}}{=} \mathbf{w}^H \mathbf{x}(t)$ corresponds to a SO estimate of a SOI coming from a particular direction and potentially corrupted by interference plus background noise, where $\mathbf{x}(t)$ is the vector of the complex envelopes of the signals observed at the output of the sensors. Although SO optimal for stationary observations, whose complex envelopes are necessarily SO circular [2], this conventional approach becomes suboptimal for nonstationary signals, omnipresent in radio communication contexts, whose complex envelope may also become SO noncircular [2] such as BPSK, ASK, MSK or GMSK signals for example. More precisely, for nonstationary observations, the optimal complex filters become time variant, and under some conditions of noncircularity, WL [3], i.e., of the form $y(t) = \mathbf{w}_1(t)^H \mathbf{x}(t) + \mathbf{w}_2(t)^H \mathbf{x}(t)^*$.

Recently, a TI WL MVDR beamformer has been introduced and deeply analyzed in [4]. However, although more powerful than the Capon's beamformer for SO noncircular interference, this WL beamformer remains suboptimal for a SO noncircular SOI, since it does not exploit the SO noncircularity of the latter. To overcome this limitation, the optimal TI WL MVDR beamformer for the reception of an unknown SOI with arbitrary noncircularity properties, corrupted by potentially SO noncircular background noise and interference has been introduced recently in [5]. This new WL MVDR beamformer takes into account the potential SO noncircularity of both the SOI and interference.

The purpose of this paper is to present a comprehensive performance analysis of this optimal WL MVDR beamformer for which only preliminary performance's study and adaptive implementations have been presented in [5]. The

paper is organized as follows. The observation model and the statement of the problem are given in Section 2. A review of the optimal WL MVDR beamformer is derived in Section 3 with its equivalent TI WL generalized sidebobe canceller (GSC) structure. The performance of this WL beamformer, in terms of both output SINR and SER, are presented in details in Sections 4 and 5 respectively.

2. HYPOTHESES, DATA STATISTICS AND PROBLEM FORMULATION

Let us consider an array of N narrow-band sensors and denote by $\mathbf{x}(t)$ the vector of complex amplitudes of the signals at the output of these sensors. Each sensor is assumed to receive a SOI corrupted by a total noise (potentially composed of interference and background noise). Under these assumptions, the observation vector $\mathbf{x}(t)$ can be written as follows

$$\mathbf{x}(t) = s(t) \mathbf{s} + \mathbf{n}(t), \quad (1)$$

where $s(t)$ and \mathbf{s} correspond to the complex envelope, assumed zero-mean and potentially SO noncircular, and the steering vector, such that its first component is equal to one, of the SOI respectively. The vector $\mathbf{n}(t)$ is the total noise vector, assumed zero-mean, potentially SO noncircular and statistically uncorrelated with $s(t)$. The SO statistics of the noncircular observation $\mathbf{x}(t)$ which are considered in this paper are defined by

$$\begin{aligned} \mathbf{R}_x &\stackrel{\text{def}}{=} \langle E[\mathbf{x}(t)\mathbf{x}(t)^H] \rangle = \pi_s \mathbf{s}\mathbf{s}^H + \mathbf{R}_n, \\ \mathbf{C}_x &\stackrel{\text{def}}{=} \langle E[\mathbf{x}(t)\mathbf{x}(t)^T] \rangle = \pi_s \gamma_s \mathbf{s}\mathbf{s}^T + \mathbf{C}_n, \end{aligned}$$

where $\langle \cdot \rangle$ denotes the time-averaging operation, with respect to the time index t , over the observation window, $\pi_s \stackrel{\text{def}}{=} \langle E[|s(t)|^2] \rangle$ is the time-averaged power of the SOI received by the first sensor, $\gamma_s \stackrel{\text{def}}{=} \langle E[s(t)^2] \rangle / \langle E[|s(t)|^2] \rangle \stackrel{\text{def}}{=} |\gamma_s| e^{2i\phi_s}$ such that $0 \leq |\gamma_s| \leq 1$, is the time-averaged SO noncircularity coefficient of the SOI, $\mathbf{R}_n \stackrel{\text{def}}{=} \langle E[\mathbf{n}(t)\mathbf{n}(t)^H] \rangle$ and $\mathbf{C}_n \stackrel{\text{def}}{=} \langle E[\mathbf{n}(t)\mathbf{n}(t)^T] \rangle$.

In order to introduce WL filters in the following, we define the extended observation vector by $\tilde{\mathbf{x}}(t) \stackrel{\text{def}}{=} [\mathbf{x}(t)^T, \mathbf{x}(t)^H]^T$ and using (1) we obtain

$$\tilde{\mathbf{x}}(t) = s(t)\tilde{\mathbf{s}}_1 + s(t)^*\tilde{\mathbf{s}}_2 + \tilde{\mathbf{n}}(t) \stackrel{\text{def}}{=} \tilde{\mathbf{S}}\tilde{\mathbf{s}}(t) + \tilde{\mathbf{n}}(t), \quad (2)$$

where $\tilde{\mathbf{n}}(t) \stackrel{\text{def}}{=} [\mathbf{n}(t)^T, \mathbf{n}(t)^H]^T$, $\tilde{\mathbf{s}}_1 \stackrel{\text{def}}{=} [\mathbf{s}^T, \mathbf{0}_N^T]^T$, $\tilde{\mathbf{s}}_2 \stackrel{\text{def}}{=} [\mathbf{0}_N^T, \mathbf{s}^H]^T$, $\tilde{\mathbf{S}} \stackrel{\text{def}}{=} [\tilde{\mathbf{s}}_1, \tilde{\mathbf{s}}_2]$ and $\tilde{\mathbf{s}}(t) \stackrel{\text{def}}{=} [s(t), s(t)^*]^T$. The SO

statistics of $\tilde{\mathbf{x}}(t)$ considered in this paper correspond to the time-averaged matrix $\mathbf{R}_{\tilde{\mathbf{x}}} \stackrel{\text{def}}{=} \langle \mathbf{E}[\tilde{\mathbf{x}}(t)\tilde{\mathbf{x}}(t)^H] \rangle$ given, under the previous assumptions, by $\mathbf{R}_{\tilde{\mathbf{x}}} = \tilde{\mathbf{S}}\mathbf{R}_s\tilde{\mathbf{S}}^H + \mathbf{R}_{\tilde{\mathbf{n}}}$ where $\mathbf{R}_{\tilde{\mathbf{s}}} \stackrel{\text{def}}{=} \langle \mathbf{E}[\tilde{\mathbf{s}}(t)\tilde{\mathbf{s}}(t)^H] \rangle$ and $\mathbf{R}_{\tilde{\mathbf{n}}} \stackrel{\text{def}}{=} \langle \mathbf{E}[\tilde{\mathbf{n}}(t)\tilde{\mathbf{n}}(t)^H] \rangle$ can be written as

$$\mathbf{R}_{\tilde{\mathbf{n}}} = \begin{pmatrix} \mathbf{R}_n & \mathbf{C}_n \\ \mathbf{C}_n^* & \mathbf{R}_n^* \end{pmatrix}. \quad (3)$$

We consider a TI WL spatial filter $\tilde{\mathbf{w}} \stackrel{\text{def}}{=} [\mathbf{w}_1^T, \mathbf{w}_2^T]^T$ whose output is defined by

$$y(t) = \tilde{\mathbf{w}}^H \tilde{\mathbf{x}}(t) = s(t)\tilde{\mathbf{w}}^H \tilde{\mathbf{s}}_1 + s(t)^* \tilde{\mathbf{w}}^H \tilde{\mathbf{s}}_2 + \tilde{\mathbf{w}}^H \tilde{\mathbf{n}}(t). \quad (4)$$

The problem is then to find the TI WL MVDR spatial filter $\tilde{\mathbf{w}}$ which generates the best SO estimate of the SOI $s(t)$, whose waveform and content are unknown.

3. OPTIMAL WL MVDR BEAMFORMERS

3.1 Optimal WL beamformer not taking into account SOI noncircularity

When γ_s is unknown, a first philosophy is to build a WL MVDR beamformer which does not require the knowledge or the estimation of this coefficient. An efficient way to generate, in the output $y(t)$, a non-null SOI without any distortion whatever the correlation between $s(t)$ and $s(t)^*$, is to minimize the time-averaged output power $\tilde{\mathbf{w}}^H \mathbf{R}_{\tilde{\mathbf{x}}} \tilde{\mathbf{w}}$ under the constraints:

$$\tilde{\mathbf{w}}^H \tilde{\mathbf{s}}_1 = 1 \quad \text{and} \quad \tilde{\mathbf{w}}^H \tilde{\mathbf{s}}_2 = 0.$$

The TI WL filter solution to this problem is the so-called WL MVDR₁ beamformer introduced and analyzed in [4] and defined by

$$\tilde{\mathbf{w}}_{\text{MVDR}_1} = \mathbf{R}_{\tilde{\mathbf{x}}}^{-1} \tilde{\mathbf{S}} [\tilde{\mathbf{S}}^H \mathbf{R}_{\tilde{\mathbf{x}}}^{-1} \tilde{\mathbf{S}}]^{-1} \mathbf{f},$$

with $\mathbf{f} \stackrel{\text{def}}{=} [1, 0]^T$. For a SO circular noise vector $\mathbf{n}(t)$, this WL beamformer reduces to the well-known Capon's MVDR beamformer defined by

$$\mathbf{w}_{\text{Capon}} \stackrel{\text{def}}{=} (\mathbf{s}^H \mathbf{R}_x^{-1} \mathbf{s})^{-1} \mathbf{R}_x^{-1} \mathbf{s}. \quad (5)$$

In the presence of SO noncircular interference sources, the WL MVDR₁ beamformer outperforms the performance of the Capon's beamformer. It is also able to process more sources than the latter in the presence of at least two rectilinear interferers. But this WL MVDR₁ beamformer does not exploit the potential SO noncircularity of the SOI. To overcome this limitation, a new WL MVDR beamformer which takes into account the potential SO noncircularity of the SOI and which is presented in Section 3.2, has been introduced in [5].

3.2 Optimal WL beamformer taking into account SOI noncircularity

For $\gamma_s \neq 0$, $s(t)^*$ is correlated with $s(t)$ and contains both a SOI and an interference component. Using an orthogonal decomposition in the Hilbert space of random processes having a finite time-averaged power and fitted with the inner product $\langle u(t), v(t) \rangle \stackrel{\text{def}}{=} \langle \mathbf{E}[u(t)v(t)^*] \rangle$, we obtain:

$$s(t)^* = \gamma_s^* s(t) + [\pi_s(1 - |\gamma_s|^2)]^{1/2} s'(t), \quad (6)$$

with $\langle \mathbf{E}[s(t)s'(t)^*] \rangle = 0$ and $\langle \mathbf{E}[|s'(t)|^2] \rangle = 1$. Decomposition (6) shows that, for a given time-averaged useful input

power π_s , the time-averaged power of the desired signal component of $s(t)^*$ is equal to $\pi_s |\gamma_s|^2$ and increases with $|\gamma_s|$. In particular for a rectilinear SOI for the receiver (BPSK, ASK), $\gamma_s = e^{2i\phi_s}$, $s(t)^* = e^{-2i\phi_s} s(t)$ and $s(t)^*$ totally corresponds to the SOI, whereas for a SO circular SOI (e.g., QPSK), $\gamma_s = 0$, $s(t)^* = \pi_s^{1/2} s'(t)$, and $s(t)^*$ totally corresponds to an interference for the SOI. Using (6) in (2), $\tilde{\mathbf{x}}(t)$ can be written as

$$\begin{aligned} \tilde{\mathbf{x}}(t) &= s(t) \underbrace{(\tilde{\mathbf{s}}_1 + \gamma_s^* \tilde{\mathbf{s}}_2)}_{\tilde{\mathbf{s}}_\gamma} + \underbrace{s'(t) [\pi_s(1 - |\gamma_s|^2)]^{1/2} \tilde{\mathbf{s}}_2 + \tilde{\mathbf{n}}(t)}_{\tilde{\mathbf{n}}_\gamma(t)} \\ &\stackrel{\text{def}}{=} s(t) \tilde{\mathbf{s}}_\gamma + \tilde{\mathbf{n}}_\gamma(t) \end{aligned} \quad (7)$$

where $\tilde{\mathbf{s}}_\gamma$ and $\tilde{\mathbf{n}}_\gamma(t)$ are the equivalent extended steering vector of the SOI, which now depends on γ_s , and the global noise vector respectively for the extended observation vector $\tilde{\mathbf{x}}(t)$. Using (7) into (4), we finally obtain

$$y(t) = \tilde{\mathbf{w}}^H \tilde{\mathbf{x}}(t) = s(t) \tilde{\mathbf{w}}^H \tilde{\mathbf{s}}_\gamma + \tilde{\mathbf{w}}^H \tilde{\mathbf{n}}_\gamma(t). \quad (8)$$

From decomposition (8), we deduce that the optimal WL MVDR beamformer, which optimally exploits the parameters \mathbf{s} and γ_s , corresponds to the WL filter $\tilde{\mathbf{w}}$ which minimizes the time-averaged output power $\tilde{\mathbf{w}}^H \mathbf{R}_{\tilde{\mathbf{x}}} \tilde{\mathbf{w}}$, under the following constraint:

$$\tilde{\mathbf{w}}^H \tilde{\mathbf{s}}_\gamma = 1. \quad (9)$$

This WL MVDR beamformer, called MVDR₂ in the following, is defined by

$$\tilde{\mathbf{w}}_{\text{MVDR}_2} \stackrel{\text{def}}{=} [\tilde{\mathbf{s}}_\gamma^H \mathbf{R}_{\tilde{\mathbf{x}}}^{-1} \tilde{\mathbf{s}}_\gamma]^{-1} \mathbf{R}_{\tilde{\mathbf{x}}}^{-1} \tilde{\mathbf{s}}_\gamma = [\tilde{\mathbf{s}}_\gamma^H \mathbf{R}_{\tilde{\mathbf{n}}_\gamma}^{-1} \tilde{\mathbf{s}}_\gamma]^{-1} \mathbf{R}_{\tilde{\mathbf{n}}_\gamma}^{-1} \tilde{\mathbf{s}}_\gamma, \quad (10)$$

where the time-averaged first correlation matrix $\mathbf{R}_{\tilde{\mathbf{n}}_\gamma}$ of $\tilde{\mathbf{n}}_\gamma(t)$ can be written from (7) as

$$\mathbf{R}_{\tilde{\mathbf{n}}_\gamma} = [\pi_s(1 - |\gamma_s|^2)] \tilde{\mathbf{s}}_2 \tilde{\mathbf{s}}_2^H + \mathbf{R}_{\tilde{\mathbf{n}}}. \quad (11)$$

We verify that the beamformer $\tilde{\mathbf{w}}_{\text{MVDR}_2}$ fits the Capon's beamformer (5) when both the SOI and the total noise are SO circular ($\gamma_s = 0$, $\mathbf{C}_n = \mathbf{O}$). Equation (8) clearly displays the SOI and the global noise uncorrelated parts of $y(t)$. It is then straightforward to introduce the SINR at the output of a WL filter $\tilde{\mathbf{w}}$ defined by

$$\text{SINR}[\tilde{\mathbf{w}}] \stackrel{\text{def}}{=} \frac{\pi_s |\tilde{\mathbf{w}}^H \tilde{\mathbf{s}}_\gamma|^2}{\tilde{\mathbf{w}}^H \mathbf{R}_{\tilde{\mathbf{n}}_\gamma} \tilde{\mathbf{w}}}, \quad (12)$$

and to prove that $\tilde{\mathbf{w}}_{\text{MVDR}_2}$ maximizes this SINR and is also proportional to $\tilde{\mathbf{w}}_{\text{MMSE}}$ which minimizes the mean square error

$$\text{MSE}[\tilde{\mathbf{w}}] \stackrel{\text{def}}{=} \langle \mathbf{E}[|s(t) - \tilde{\mathbf{w}}^H \tilde{\mathbf{x}}(t)|^2] \rangle. \quad (13)$$

3.3 Equivalent TI WL GSC structure

It can be easily verified that the WL beamformer MVDR₂ has an equivalent WL GSC structure [6] depicted on Fig.1. $\tilde{\mathbf{w}}_0$ is a deterministic WL spatial filter such that $\tilde{\mathbf{w}}_0^H \tilde{\mathbf{s}}_\gamma = 1$, whose output is given by $y_0(t) = \tilde{\mathbf{w}}_0^H \tilde{\mathbf{x}}(t)$. \mathbf{B}^H is full rank $(2N - 1) \times 2N$ blocking matrix verifying $\mathbf{B}^H \tilde{\mathbf{s}}_\gamma = \mathbf{0}$, whose output $\mathbf{B}^H \tilde{\mathbf{x}}$ corresponds to the vector $\tilde{\mathbf{z}}(t)$. $\tilde{\mathbf{w}}_a$ is a WL spatial filter which generates the output $y_a(t) = \tilde{\mathbf{w}}_a^H \tilde{\mathbf{z}}(t)$ and which minimizes the time-averaged power of the output $y(t) = y_0(t) - y_a(t)$.

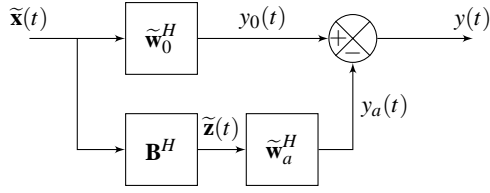


Fig.1 Equivalent WL MVDR₂ GSC structure.

4. SINR PERFORMANCE ANALYSIS

4.1 General SINR analysis

For a given source scenario, it is easy to compare the SINR at the output of the Capon, MVDR₁ and MVDR₂ beamformers without any particular computations. Indeed, $\mathbf{w}_{\text{Capon}}$, $\tilde{\mathbf{w}}_{\text{MVDR}_1}$ and $\tilde{\mathbf{w}}_{\text{MVDR}_2}$, all minimize the time-averaged output power $\tilde{\mathbf{w}}^H \mathbf{R}_s \tilde{\mathbf{w}}$ but under different constraints that satisfy

$$\begin{aligned} \{\tilde{\mathbf{w}} = [\mathbf{w}_1^T, \mathbf{0}_N^T]^T; \mathbf{w}_1^H \mathbf{s} = 1\} \\ \subset \{\tilde{\mathbf{w}}; \tilde{\mathbf{w}}^H \tilde{\mathbf{s}}_1 = 1 \text{ and } \tilde{\mathbf{w}}^H \tilde{\mathbf{s}}_2 = 0\} \subset \{\tilde{\mathbf{w}}; \tilde{\mathbf{w}}^H \tilde{\mathbf{s}}_\gamma = 1\}. \end{aligned}$$

Consequently, the inclusion principle implies that generally

$$\text{SINR}_{\text{Capon}} \leq \text{SINR}_{\text{MVDR}_1} \leq \text{SINR}_{\text{MVDR}_2}. \quad (14)$$

Let us now analyze the variation of $\text{SINR}_{\text{MVDR}_2}$ with respect to γ_s . Using $\tilde{\mathbf{w}} = \tilde{\mathbf{w}}_{\text{MVDR}_2}$ defined by (10), in (12), the SINR at the output of the MVDR₂ beamformer is given by

$$\text{SINR}_{\text{MVDR}_2} = \pi_s \tilde{\mathbf{s}}_\gamma^H \mathbf{R}_{n_\gamma}^{-1} \tilde{\mathbf{s}}_\gamma. \quad (15)$$

From (3), $\mathbf{R}_{\tilde{n}}^{-1}$ can be written as

$$\mathbf{R}_{\tilde{n}}^{-1} = \begin{pmatrix} \mathbf{A} & \mathbf{D} \\ \mathbf{D}^* & \mathbf{A}^* \end{pmatrix} \text{ with } \begin{aligned} \mathbf{A} &= (\mathbf{R}_n - \mathbf{C}_n \mathbf{R}_n^{*-1} \mathbf{C}_n^*)^{-1} \\ \mathbf{D} &= -\mathbf{A} \mathbf{C}_n \mathbf{R}_n^{*-1}. \end{aligned}$$

Then, applying the Inversion Lemma to (11) and substituting the previous expressions into (15), we obtain after simple algebraic manipulations

$$\begin{aligned} \text{SINR}_{\text{MVDR}_2} &= \pi_s \left(\mathbf{s}^H \mathbf{A} \mathbf{s} (1 + |\gamma_s|^2) + 2\Re(\gamma_s^* \mathbf{s}^H \mathbf{D} \mathbf{s}^*) \right. \\ &\quad \left. - \frac{|\mathbf{s}^H \mathbf{D} \mathbf{s}^* + \gamma_s \mathbf{s}^H \mathbf{A} \mathbf{s}|^2}{[\pi_s (1 - |\gamma_s|^2)]^{-1} + \mathbf{s}^H \mathbf{A} \mathbf{s}} \right). \quad (16) \end{aligned}$$

For a SO circular SOI ($\gamma_s = 0$), (16) gives

$$\text{SINR}_{\text{MVDR}_2} = \pi_s \left(\mathbf{s}^H \mathbf{A} \mathbf{s} - \frac{|\mathbf{s}^H \mathbf{D} \mathbf{s}^*|}{\pi_s^{-1} + \mathbf{s}^H \mathbf{A} \mathbf{s}} \right),$$

which has been given for the first time in [7] with the MMSE criterion, which is always greater than $\text{SINR}_{\text{MVDR}_1}$ [4] and which tends to $\text{SINR}_{\text{MVDR}_1}$ when $\pi_s \mathbf{s}^H \mathbf{A} \mathbf{s} \gg 1$.

For a rectilinear SOI ($|\gamma_s| = 1$), (16) gives

$$\begin{aligned} \text{SINR}_{\text{MVDR}_2} &= 2\pi_s (\mathbf{s}^H \mathbf{A} \mathbf{s} + \Re(e^{-2i\phi_s} \mathbf{s}^H \mathbf{D} \mathbf{s}^*)) \\ &= 2\pi_s (\mathbf{s}^H \mathbf{A} \mathbf{s} - |\mathbf{s}^H \mathbf{D} \mathbf{s}^*| \cos(2\phi)) \end{aligned}$$

where $2\phi \stackrel{\text{def}}{=} \phi_{d_s} - 2\phi_s + \pi$ with $\phi_{d_s} \stackrel{\text{def}}{=} \text{Arg}(d_s)$, with $d_s \stackrel{\text{def}}{=} \mathbf{s}^H \mathbf{D} \mathbf{s}^*$. This expression corresponds to the SINR at the output of the optimal receiver analyzed in [8].

For arbitrary values of $|\gamma_s|$, two cases must be distinguished:

If $d_s = 0$, which occurs in particular for a SO circular total noise ($\mathbf{C}_n = \mathbf{O}$) or when \mathbf{s}^* is in the kernel of \mathbf{D} , it is straightforward to prove from (16) that $\text{SINR}_{\text{MVDR}_2}$ is an increasing function of $|\gamma_s|$. The minimal value of $\text{SINR}_{\text{MVDR}_2}$

obtained for $\gamma_s = 0$ corresponds to $\pi_s \mathbf{s}^H \mathbf{R}_n^{-1} \mathbf{s} = \text{SINR}_{\text{Capon}}$, whereas its maximal value is obtained for $|\gamma_s| = 1$ and corresponds to $2\pi_s \mathbf{s}^H \mathbf{R}_n^{-1} \mathbf{s} = 2\text{SINR}_{\text{Capon}}$.

Now if $d_s \neq 0$, which occurs for a SO noncircular total noise ($\mathbf{C}_n \neq \mathbf{O}$) provided that \mathbf{s}^* is not in the kernel of \mathbf{D} , the variation study of $\text{SINR}_{\text{MVDR}_2}$ with $|\gamma_s|$ is more intricate. We can prove that $\text{SINR}_{\text{MVDR}_2}$ is an increasing function of $|\gamma_s|$ for $\cos(2\phi) \leq 0$, whereas for $\cos(2\phi) > 0$, there exists a value of $|\gamma_s|$ noted $|\gamma_{s,\text{min}}|$, such that $\text{SINR}_{\text{MVDR}_2}$ decreases for $0 \leq |\gamma_s| \leq |\gamma_{s,\text{min}}|$ and increases for $|\gamma_{s,\text{min}}| \leq |\gamma_s| \leq 1$. This shows in this case the existence of a parameter $0 < |\gamma_{s,\text{min}}| < 1$ which minimizes $\text{SINR}_{\text{MVDR}_2}$.

4.2 SINR for one interference source

In the presence of a single interference source,

$$\mathbf{R}_n = \pi_1 \mathbf{j}_1 \mathbf{j}_1^H + \eta_2 \mathbf{I} \quad \text{and} \quad \mathbf{C}_n = \pi_1 \gamma_1 \mathbf{j}_1 \mathbf{j}_1^T,$$

where $\gamma_1 \stackrel{\text{def}}{=} |\gamma_1| e^{2i\phi_1}$ is the time-averaged SO noncircularity coefficient of the interference. Then, $\text{SINR}_{\text{MVDR}_2}$ can be computed and compared with the SINR at the output of the Capon and MVDR₁ beamformers.

4.2.1 Case of a rectilinear SOI ($|\gamma_s| = 1$) and a strong interference

For a rectilinear SOI and a rectilinear interference which is assumed to be strong (i.e., $\varepsilon_1 \stackrel{\text{def}}{=} (\mathbf{j}_1^H \mathbf{j}_1) \pi_1 / \eta_2 \gg 1$), $\text{SINR}_{\text{MVDR}_2}$ becomes

$$\text{SINR}_{\text{MVDR}_2} \approx 2\varepsilon_s (1 - |\alpha_{1s}|^2 \cos^2(\phi)), \quad (17)$$

whereas $\text{SINR}_{\text{Capon}}$ and $\text{SINR}_{\text{MVDR}_1}$ are given by

$$\text{SINR}_{\text{Capon}} \approx \varepsilon_s (1 - |\alpha_{1s}|^2), \quad |\alpha_{1s}| \neq 1 \quad (18)$$

$$\text{SINR}_{\text{MVDR}_1} \approx \varepsilon_s \left(1 - \frac{|\alpha_{1s}|^2}{2 - |\alpha_{1s}|^2} \right), \quad |\alpha_{1s}| \neq 1. \quad (19)$$

In these expressions $\varepsilon_s \stackrel{\text{def}}{=} (\mathbf{s}^H \mathbf{s}) \pi_s / \eta_2$ and $\alpha_{1s} \stackrel{\text{def}}{=} \mathbf{j}_1^H \mathbf{s} / (\mathbf{j}_1^H \mathbf{j}_1)^{1/2} (\mathbf{s}^H \mathbf{s})^{1/2}$. Expression (17), which has been obtained in [8], shows in this case that the MVDR₂ beamformer discriminates sources by both direction of arrival (DOA) (for $N > 1$) and phase, allowing in particular single antenna interference cancellation (SAIC), contrary to the Capon and MVDR₁ beamformer which can discriminate sources only by the DOA (for $N > 1$).

For rectilinear SOI and a strong non rectilinear interference, provided $|\alpha_{1s}| \neq 1$, $\text{SINR}_{\text{MVDR}_1} \approx \text{SINR}_{\text{Capon}}$ given by (18), whereas $\text{SINR}_{\text{MVDR}_2} \approx 2 \text{SINR}_{\text{Capon}}$. In this case, $\text{SINR}_{\text{MVDR}_2}$ is twice the SINR at the output of Capon and MVDR₁ beamformers due to the exploitation of the noncircularity of the SOI.

4.2.2 Case of a non rectilinear SOI ($|\gamma_s| \neq 1$) and a strong interference

For a non rectilinear SOI and a strong rectilinear interference, $\text{SINR}_{\text{Capon}}$ and $\text{SINR}_{\text{MVDR}_1}$ are still given by (18) and (19) respectively, whereas $\text{SINR}_{\text{MVDR}_2}$ becomes

$$\begin{aligned} \text{SINR}_{\text{MVDR}_2} \approx \varepsilon_s \left([(2 - |\alpha_{1s}|^2)(1 + |\gamma_s|^2) + 2\varepsilon_s (1 - |\alpha_{1s}|^2)(1 - |\gamma_s|^2)] \right. \\ \left. - 2|\alpha_{1s}|^2 |\gamma_s| \cos(2\phi) \right) / [2 + \varepsilon_s (2 - |\alpha_{1s}|^2)(1 - |\gamma_s|^2)] \end{aligned}$$

for arbitrary α_{1s} . In particular for a strong ($\varepsilon_s \gg 1$) circular SOI ($\gamma_s = 0$), $\text{SINR}_{\text{MVDR}_2} \approx 1$ for $|\alpha_{1s}| = 1$, whereas $\text{SINR}_{\text{MVDR}_2} \approx \text{SINR}_{\text{MVDR}_1}$ for $|\alpha_{1s}| \neq 1$ given by (19).

Finally, for a non rectilinear SOI and a strong non rectilinear interference $\text{SINR}_{\text{MVDR}_1} \approx \text{SINR}_{\text{Capon}}$ given by (18), whereas $\text{SINR}_{\text{MVDR}_2}$ is given by

$$\text{SINR}_{\text{MVDR}_2} \approx \left(1 + \frac{|\gamma_s|^2}{1 + \varepsilon_s (1 - |\gamma_s|^2)(1 - |\alpha_{1s}|^2)} \right) \text{SINR}_{\text{Capon}},$$

for $|\alpha_{1s}| \neq 1$. In this case $\text{SINR}_{\text{MVDR}_2}$ is an increasing function of $|\gamma_s|$ varying from $\text{SINR}_{\text{Capon}}$ obtained for a circular SOI to 2 $\text{SINR}_{\text{Capon}}$ obtained for a rectilinear SOI.

4.2.3 Illustrations

To illustrate the previous results, we consider that an array of $N = 2$ omnidirectional sensors, equispaced half a wavelength apart, receives a SOI, an interference and a background noise, whose DOAs are equal to $\pi/3$ and $\pi/2$ respectively and such that $\pi_s/\eta_2 = 10$ dB and $\pi_1/\eta_2 = 20$ dB. Note that for a single interference, $2\phi = 2(\phi_1 - \phi_s - \phi_{1s})$, where ϕ_{1s} is phase argument of α_{1s} , which means that ϕ corresponds to the phase diversity between the interference and the SOI for the considered array. Under these assumptions, Fig.2 (a) and 2 (b) show the variations of $\text{SINR}_{\text{Capon}}$, $\text{SINR}_{\text{MVDR}_1}$ and $\text{SINR}_{\text{MVDR}_2}$ as a function of $|\gamma_s|$ for $\phi = 6\pi/15$ ($\cos(2\phi) < 0$) and $\phi = \pi/15$ ($\cos(2\phi) > 0$) respectively, for two different values of $|\gamma_1|$ (1 or 0.9). We note the constant values of $\text{SINR}_{\text{Capon}}$ and $\text{SINR}_{\text{MVDR}_1}$ as $|\gamma_s|$ increases. We also note the increasing value of $\text{SINR}_{\text{MVDR}_2}$ with $|\gamma_s|$ for $\cos(2\phi) < 0$ and the existence of a value, $0 \leq |\gamma_{s,\min}| \leq 1$ of $|\gamma_s|$, which minimizes $\text{SINR}_{\text{MVDR}_2}$ for $\cos(2\phi) > 0$. We note in both cases, the increasing value of $\text{SINR}_{\text{MVDR}_1}$ and $\text{SINR}_{\text{MVDR}_2}$ as $|\gamma_1|$ increases.

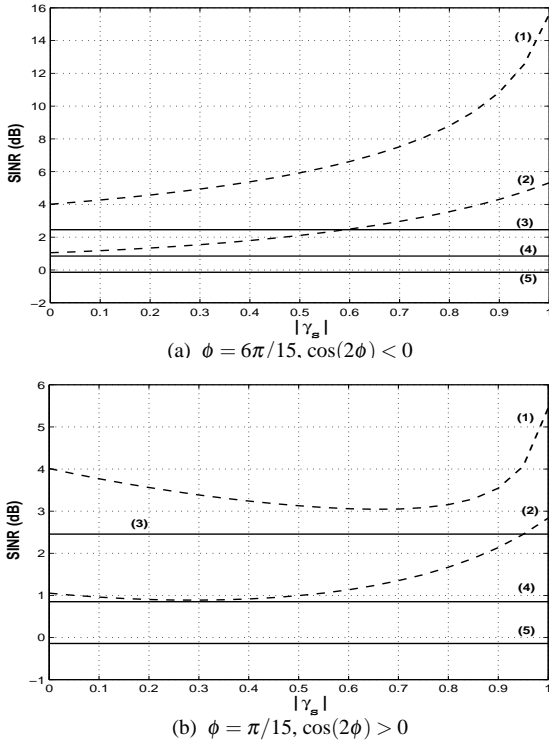


Fig.2 $\text{SINR}_{\text{Capon}}$, $\text{SINR}_{\text{MVDR}_1}$ and $\text{SINR}_{\text{MVDR}_2}$ as a function of $|\gamma_s|$, (1) (MVDR₂ $|\gamma_1| = 1$), (2) (MVDR₂ $|\gamma_1| = 0.9$), (3) (MVDR₁ $|\gamma_1| = 1$), (4) (MVDR₁ $|\gamma_1| = 0.9$), (5) $\text{SINR}_{\text{Capon}}$.

4.3 SINR and MSE

Using decomposition (4) and the general expressions (12) and (13) of the SINR and MSE, the following relation be-

tween the MSE and SINR criteria is easily proved.

$$\text{MSE}[\tilde{\mathbf{w}}] = \pi_s \left(|1 - \tilde{\mathbf{w}}^H \tilde{\mathbf{s}}_\gamma|^2 + \frac{|\tilde{\mathbf{w}}^H \tilde{\mathbf{s}}_\gamma|^2}{\text{SINR}[\tilde{\mathbf{w}}]} \right).$$

This relation is interesting since it shows that the WL filter $\tilde{\mathbf{w}}$ which minimizes $\text{MSE}[\tilde{\mathbf{w}}]$ under the constraint $\tilde{\mathbf{w}}^H \tilde{\mathbf{s}}_\gamma = 1$, is also the WL filter which maximizes $\text{SINR}[\tilde{\mathbf{w}}]$ under the same constraint, which finally corresponds to $\tilde{\mathbf{w}}_{\text{MVDR}_2}$. This shows that, for WL filters verifying constraint (9), the introduced SINR corresponds, to within a constant term, to the inverse of the MSE.

5. SER PERFORMANCE ANALYSIS

In applications such as passive listening, the SOI waveform is unknown, which prevents from implementing the optimal WL receiver for demodulation purposes and which justifies the approach considered in both [4] and this paper, valid whatever the kind of SOI (digital or not). However, despite of this fact and for a digital SOI, it is always possible to compute and to analyze the SER after demodulation from the output of Capon, MVDR₁ or MVDR₂ beamformer. Such an analyze allows to evaluate the pertinence of the chosen SINR criterion to optimize the reception of noncircular SOI with unknown waveform in the presence of noncircular interferences. More precisely, let us consider a linearly modulated SOI corrupted by a single linearly modulated interference and a Gaussian background noise. To simplify the analysis, we assume that the SOI and interference have common 1/2 Nyquist pulse shapes, carriers and symbol rates and furthermore are perfectly synchronized. In the absence of frequency offset, assuming an ideal symbol rate sampling so that intersymbol interference is removed at the output of a matched filter to the pulse shaped filter, the sampled observation vector at the output of this filter can be written as

$$\mathbf{x}_v(kT) = s_k \mathbf{s} + j_k \mathbf{j}_1 + \mathbf{n}'(kT), \quad (20)$$

where T is the symbol period, $s_k = \sqrt{\pi_s} e^{i\phi_s} a_k$, $j_k = \sqrt{\pi_1} e^{i\phi_1} b_k$, a_k and b_k are the SOI and interference symbols, and where $\mathbf{n}'(kT)$ is an N -variate zero-mean circular Gaussian random variable with $\text{E}(\mathbf{n}'(kT)\mathbf{n}'(kT)^H) = \eta_2 \mathbf{I}$.

In order to derive simple closed-form expressions of the SER at the output of the considered beamformers, we only consider in the following, the case of equiprobable BPSK ($\{-1, +1\}$) and QPSK ($\{\pm 1, \pm i\}$) symbols for the SOI and interference source. In the case of both QPSK SOI and interference source, the MVDR₂ beamformer reduces to the Capon beamformer, so we only examine the SER in the three following situations: both SOI and interference source are BPSK, the SOI is BPSK and the interference source is QPSK, and the SOI is QPSK and the interference source is BPSK for which the outputs, $y(kT) = \tilde{\mathbf{w}}^H \tilde{\mathbf{x}}(kT)$, of a given WL beamformer $\tilde{\mathbf{w}}$ are respectively given by

$$\begin{aligned} y(kT) &= c_s a_k + c_1^1 b_k + n_k, \\ y(kT) &= c_s a_k + c_1^2 b_k + c_1^3 b_k^* + n_k, \\ y(kT) &= c_s a_k + c_s' a_k^* + c_1^1 b_k + n_k, \end{aligned}$$

where $c_s = \sqrt{\pi_s} e^{i\phi_s}$, $c_1^1 = \sqrt{\pi_1} e^{i\phi_1} \tilde{\mathbf{w}}^H \tilde{\mathbf{j}}_\gamma$ with $\tilde{\mathbf{j}}_\gamma \stackrel{\text{def}}{=} (\mathbf{j}_1^T, e^{-2i\phi_1} \mathbf{j}_1^H)^T$, $c_1^2 = \sqrt{\pi_1} e^{i\phi_1} \tilde{\mathbf{w}}^H \tilde{\mathbf{j}}_1$ with $\tilde{\mathbf{j}}_1 \stackrel{\text{def}}{=} (\mathbf{j}_1^T, \mathbf{0}_N^T)^T$, $c_1^3 = \sqrt{\pi_1} e^{-i\phi_1} \tilde{\mathbf{w}}^H \tilde{\mathbf{j}}_2$ with $\tilde{\mathbf{j}}_2 \stackrel{\text{def}}{=} (\mathbf{0}_N^T, \mathbf{j}_1^H)^T$, $c_s' = \sqrt{\pi_s} e^{-i\phi_s} \tilde{\mathbf{w}}^H \tilde{\mathbf{s}}_2$ and $n_k = \tilde{\mathbf{w}}^H \tilde{\mathbf{n}}'(kT)$.

For both BPSK SOI and interference, using the following MLSE receiver (under the false assumption of circular Gaussian total noise at the output of the output $y(kT)$)

$$\hat{a}_k = \text{Sign}[\Re(c_s^* y(kT))], \quad (21)$$

we obtain by conditioning with respect to the interference symbols

$$\text{SER} = \frac{1}{2} \left\{ Q(\sqrt{\text{SNR}} + \sqrt{\text{INR}}) + Q(\sqrt{\text{SNR}} - \sqrt{\text{INR}}) \right\}, \quad (22)$$

with $\text{SNR} = \frac{\pi_s}{2\eta_2 \|\tilde{\mathbf{w}}\|^2}$ and $\text{INR} = \frac{2\pi_1 [\Re(e^{i(\phi_1 - \phi_s)} \mathbf{w}^H \mathbf{j}_1)]^2}{\eta_2 \|\tilde{\mathbf{w}}\|^2}$ with $\tilde{\mathbf{w}} = (\mathbf{w}^T, e^{-2i\phi_s} \mathbf{w}^H)^T$ and where $Q(v) \stackrel{\text{def}}{=} \int_v^{+\infty} \frac{1}{\sqrt{2\pi}} e^{-u^2/2} du$. Note that expression (22) has been obtained in [8].

For BPSK SOI and QPSK interference, using receiver (21), which is still the MLSE receiver under the false assumption of circular Gaussian total noise at the output of the output $y(kT)$, we obtain in the same way

$$\begin{aligned} \text{SER} &= \frac{1}{4} \left\{ Q(\sqrt{\text{SNR}_1} + \sqrt{\text{INR}_1}) + Q(\sqrt{\text{SNR}_1} - \sqrt{\text{INR}_1}) \right\} \\ &\quad + \frac{1}{4} \left\{ Q(\sqrt{\text{SNR}_2} + \sqrt{\text{INR}_2}) + Q(\sqrt{\text{SNR}_2} - \sqrt{\text{INR}_2}) \right\}, \end{aligned}$$

with $\text{SNR}_\ell = \frac{2\pi_s}{\eta_2 [\|\tilde{\mathbf{w}}\|^2 + 2\Re(e^{2i\phi_s} \mathbf{w}_\ell^T \mathbf{w}_2)]}$ and $(\text{INR}_\ell)_{\ell=1,2} = \frac{2\pi_1 [\Re(i^{\ell-1} e^{i(\phi_1 - \phi_s)} \mathbf{w}_\ell^T \mathbf{j}_1) - (-1)^\ell \Re(i^{\ell-1} e^{-i(\phi_1 + \phi_s)} \mathbf{w}_\ell^T \mathbf{j}_1^*)]}{\eta_2 [\|\tilde{\mathbf{w}}\|^2 + 2\Re(e^{2i\phi_s} \mathbf{w}_\ell^T \mathbf{w}_2)]}$ with $\tilde{\mathbf{w}} \stackrel{\text{def}}{=} (\mathbf{w}_1^T, \mathbf{w}_2^T)^T$.

We note that the terms SNR, SNR₁ and INR, INR₁, INR₂ are respectively proportional to the ratios π_s/η_2 and π_1/η_2 , which justifies the notations signal-to-noise ratio (SNR) and signal-to-interference ratio (INR), but all these terms also depend on π_s, π_1, η_2 through $\tilde{\mathbf{w}}$ which satisfies constraint (9).

Finally for QPSK SOI and BPSK interference, using the following receiver which is still the MLSE receiver under the false assumption of circular Gaussian total noise at the output of the output $y(kT)$,

$$\hat{a}_k = \text{Arg}(\text{Min}_{\alpha \in \{\pm 1, \pm i\}} |y(kT) - c_s \alpha|),$$

with four decision areas in \mathbb{C} for $c_s^* y(kT)$, we obtain

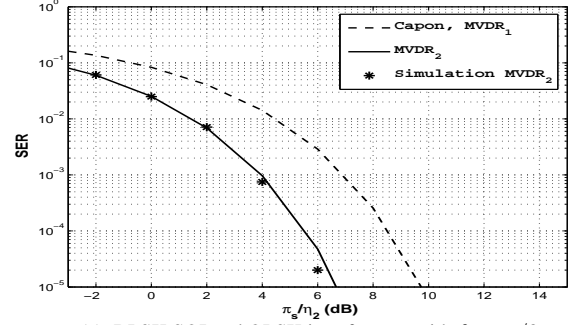
$$\text{SER} = \frac{1}{2} \left\{ Q'(\Delta_1, \tilde{\mathbf{R}}) + Q'(\Delta_2, \tilde{\mathbf{R}}) \right\},$$

where $Q'(\Delta_\ell, \tilde{\mathbf{R}}) \stackrel{\text{def}}{=} \int_{\Delta_\ell} p(z, \tilde{\mathbf{R}}) dx dy$ with $z = x + iy$ and $p(z, \tilde{\mathbf{R}}) = \frac{1}{\pi \sqrt{\det(\tilde{\mathbf{R}})}} e^{-\tilde{\mathbf{z}}^H \tilde{\mathbf{R}}^{-1} \tilde{\mathbf{z}}/2}$ where $\tilde{\mathbf{z}} \stackrel{\text{def}}{=} (z, z^*)^T$,

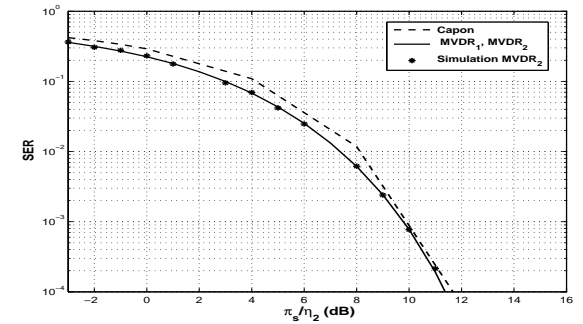
$\tilde{\mathbf{R}} = \pi_s \eta_2 \begin{pmatrix} \|\tilde{\mathbf{w}}\|^2 & 2e^{-2i\phi_s} \mathbf{w}_2^H \mathbf{w}_1^* \\ 2e^{2i\phi_s} \mathbf{w}_2^T \mathbf{w}_1 & \|\tilde{\mathbf{w}}\|^2 \end{pmatrix}$ is the covariance matrix of the noncircular Gaussian distributed vector $(c_s^* n_k, c_s n_k^*)^T$, and $(\Delta_\ell)_{\ell=1,2} \stackrel{\text{def}}{=} \{z + \alpha_\ell \in \Delta\}$ with $\Delta \stackrel{\text{def}}{=} \{z = |z|^{i\theta} \in \mathbb{C}; |\theta| \leq 3\pi/4\}$ and $\alpha_\ell \stackrel{\text{def}}{=} -\pi_s - \pi_s e^{-2i\phi_s} \mathbf{w}_2^H \mathbf{s}^* - (-1)^\ell \sqrt{\pi_s \pi_1} [e^{i(\phi_1 - \phi_s)} \mathbf{w}_1^H \mathbf{j} + e^{i(\phi_1 + \phi_s)} \mathbf{w}_2^H \mathbf{j}^*]$, $\ell = 1, 2$.

Fig.3a and 3b illustrate the variations of the SER at the output of Capon, MVDR₁ and MVDR₂ beamformers, as a function of SNR for (a) BPSK SOI and QPSK interference source and (b) QPSK SOI and BPSK interference source. For the MVDR₂ beamformer, both theoretical and estimated (from 1000 observed errors) values of SER are computed. Fig.3a and 3b show the good agreement of theoretical results with respect to estimated ones. Moreover, although the SER is not the criterion which is optimized by the WL MVDR₂, it is improved by the latter with respect to the one at the output of Capon and WL MVDR₁ beamformer, whatever the non-circularity of the SOI.

Finally, we note that the SER and SINR behaviors are consistent because for these parameters, the MVDR₂ beamformer outperforms the Capon and MVDR₁ beamformers for both SINR and SER points of view by 3dB for BPSK SOI and QPSK interference source, whereas, the MVDR₁ and MVDR₂ beamformers outperform the Capon beamformer for both SINR and SER point of view by about 1.2dB for QPSK SOI and BPSK interference source.



(a) BPSK SOI and QPSK interference with $\theta_1 = \pi/3$



(b) QPSK SOI and BPSK interference source with $\theta_1 = \pi/6$

Fig.3 Theoretical and estimated SER as a function of π_s/η_2 for $N = 2$, $\pi_1/\eta_2 = 10\text{dB}$, $\phi_s = 0$, $\phi_1 = \pi/4$ and $\theta_s = 0$ for Capon, MVDR₁ and MVDR₂ beamformers.

REFERENCES

- [1] P. Chevalier, "Optimal array processing for nonstationary signals", *Proc. ICASSP*, pp. 2868-2871, Atlanta, USA, May 1996.
- [2] B. Picinbono, "On Circularity", *IEEE Trans. Signal Process.*, vol. 42, no. 12, pp. 3473-3482, Dec 1994.
- [3] B. Picinbono and P. Chevalier, "Widely linear estimation with complex data", *IEEE Trans. Signal Process.*, vol. 43, no. 8, pp. 2030-2033, Aug. 1995.
- [4] P. Chevalier and A. Blin, "Widely linear MVDR beamformers for the reception of an unknown signal corrupted by noncircular interferences", *IEEE Trans. Signal Process.*, vol. 55, no. 11, pp. 5323-5336, Nov 2007.
- [5] P. Chevalier, J.P. Delmas and A. Oukaci, "Optimal widely linear MVDR beamforming for noncircular signals", accepted to *ICASSP*, Taipei, Taiwan, 2009.
- [6] L.J. Griffiths and C.W. Jim, "An alternative approach to linearly constrained adaptive beamforming", *IEEE Trans. Ant. Prop.*, vol. 30, no. 1, pp. 27-34, Jan. 1982.
- [7] P. Chevalier, "Optimal time invariant and widely linear spatial filtering for radiocommunications", *Proc. EUSIPCO*, pp. 559-562, Trieste (Italy), Sept. 1996.
- [8] P. Chevalier and F. Pipon, "New Insights into optimal widely linear array receivers for the demodulation of BPSK, MSK and GMSK signals corrupted by noncircular interferences - Application to SAIC", *IEEE Trans. Signal Process.*, vol. 54, no. 3, pp. 870-883, March 2006.